

Interactions between Antimicrobial Polynorbornenes and Phospholipid Vesicles Monitored by Light Scattering and Microcalorimetry

Gregory J. Gabriel, Joanna G. Pool, Abhigyan Som, Jeffrey M. Dabkowski, E. Bryan Coughlin, M. Muthukumar, and Gregory N. Tew*

Department of Polymer Science and Engineering, University of Massachusetts, Amherst, 120 Governors Drive, Amherst, Massachusetts 01003

Received July 12, 2008. Revised Manuscript Received September 3, 2008

Antimicrobial polynorbornenes composed of facially amphiphilic monomers have been previously reported to accurately emulate the antimicrobial activity of natural host-defense peptides (HDPs). The lethal mechanism of most HDPs involves binding to the membrane surface of bacteria leading to compromised phospholipid bilayers. In this paper, the interactions between biomimetic vesicle membranes and these cationic antimicrobial polynorbornenes are reported. Vesicle dye-leakage experiments were consistent with previous biological assays and corroborated a mode of action involving membrane disruption. Dynamic light scattering (DLS) showed that these antimicrobial polymers cause extensive aggregation of vesicles without complete bilayer disintegration as observed with surfactants that efficiently solubilize the membrane. Fluorescence microscopy on vesicles and bacterial cells also showed polymer-induced aggregation of both synthetic vesicles and bacterial cells. Isothermal titration calorimetry (ITC) afforded free energy of binding values (ΔG) and polymer to lipid binding ratios, plus revealed that the interaction is entropically favorable ($\Delta S > 0$, $\Delta H > 0$). It was observed that the strength of vesicle binding was similar between the active polymers while the binding stoichiometries were dramatically different.

Introduction

In ongoing efforts to elucidate design parameters for potent antimicrobial polymers, a series of amphiphilic polynorbornenes was previously synthesized and reported to possess tunable antimicrobial and hemolytic activities (Figure 1).¹ Here, we investigate the fundamental interactions of these polymers with synthetic biomimetic vesicles by several different techniques since it was proposed that these types of polymers kill bacteria by disrupting the cellular membrane. Specifically, we employed vesicle dye-leakage assays, dynamic light scattering (DLS), fluorescence microscopy and isothermal titration calorimetry (ITC) to study polymer/membrane interactions.

Membrane interactions of host-defense peptides (HDPs)^{2–4} have been previously characterized by DLS and ITC. In many cases, their antimicrobial mode of action has been attributed to these membrane interactions.^{5–8} However, synthetic mimics of antimicrobial peptides (SMAMPs) have not yet been fundamentally studied by these two particular techniques.⁹ Inherent challenges were anticipated in monitoring the vesicle interactions of higher molecular weight (~ 10 kDa) polydisperse samples in contrast to the previously studied individual HDPs which are smaller (< 4 kDa) and monodisperse.

The field of antimicrobial polymers has experienced fast growth in large part due to the pressing need for nontoxic materials

resistant to Biofilm formation.^{10,11} For example, bacterial-infected implants are an extremely costly problem (in terms of dollar amount and patient suffering) and is sure to get worse with an aging population in addition to the emergence of more antibiotic-resistant bacterial strains.^{12,13} Inexpensive antifouling materials for boat hulls, as another example, would be an effective cost-cutting measure for the shipping industry. Other applications for antimicrobial polymers include novel therapeutics, permanently sterile coatings, water purifying membranes, and disinfectant additives such as the commercially used poly(hexamethylene biguanides).¹⁰

The design for polynorbornenes **1–4** (Figure 1) was inspired in part by the facially amphiphilic (FA) structure of many HDPs. They display their cationic and nonpolar residues on opposite faces of their folded conformation or secondary structure; in other words they attain an FA conformation either in solution or induced by a biological membrane. There have been several examples of antimicrobial proteomimetics reported in which an FA solution structure, whether it be an α -helix or a β -sheet secondary structure, was not required for membrane-disruption activity.^{14–19} It is thought that if a sufficiently flexible macromolecule can segregate their charged and nonpolar moieties effectively during (and not necessarily before) interaction at the membrane interface, then membrane-disruption and subsequent cell death may occur.²⁰ While secondary structure was not designed into the polymers in this study, the monomer units

* To whom correspondence should be addressed. E-mail: tew@mail.pse.umass.edu.

(1) Ilker, M. F.; Nüsslein, K.; Tew, G. N.; Coughlin, E. B. *J. Am. Chem. Soc.* **2004**, *126*, 15870–15875.

(2) Zasloff, M. *Nature* **2002**, *415*, 389–395.

(3) Brogden, K. A. *Nat. Rev. Microbiol.* **2005**, *3*, 238–250.

(4) Zhang, L.; Rozek, A.; Hancock, R. E. *J. Biol. Chem.* **2001**, *276*, 35714–35722.

(5) Abraham, T.; Lewis, R. N. A. H.; Hodges, R. S.; McElhaney, R. N. *Biochemistry* **2005**, *44*, 11279–11285.

(6) Wieprecht, T.; Apostolov, O.; Beyermann, M.; Seelig, J. *Biochemistry* **2000**, *39*, 442–452.

(7) Wieprecht, T.; Beyermann, M.; Seelig, J. *Biochemistry* **1999**, *38*, 10377–10387.

(8) Wieprecht, T.; Apostolov, O.; Seelig, J. *Biophys. Chem.* **2000**, *85*, 187–198.

(9) (a) Several X-ray techniques have been used to study a series of short synthetic antimicrobial oligomers and their interactions with membranes. See: Yang, L.; Gordon, V. D.; Mischra, A.; Som, A.; Purdy, K. R.; Davis, M. A.; Tew, G. N.; Wong, G. C. L. *J. Am. Chem. Soc.* **2007**, *129*, 12141–12147. (b) Ishitsuka, Y.; Arnt, L.; Ratajczek, M.; Frey, S.; Majewski, J.; Kjaer, K.; Tew, G. N.; Lee, K. Y. C. *J. Am. Chem. Soc.* **2006**, *128*, 13123–13129.

(10) Gabriel, G. J.; Som, A.; Madkour, A. E.; Eren, T.; Tew, G. N. *Mater. Sci. Eng., R: Reports*, **R57** **2007**, *R57*, 28–64.

(11) Kenawy, E. R.; Worley, S. D.; Broughton, R. *Biomacromolecules* **2007**, *8*, 1359–1384.

(12) Hetrick, E. M.; Schoenfisch, M. H. *Chem. Soc. Rev.* **2006**, *35*, 780–789.

(13) Darouiche, R. O. *N. Engl. J. Med.* **2004**, *350*, 1422–1429.

(14) Tew, G. N.; Liu, D.; Chen, B.; Doerksen, R. J.; Kaplan, J.; Carroll, P. J.; Klein, M. L.; DeGrado, W. F. *Proc. Natl. Acad. Sci. U.S.A.* **2002**, *99*, 5110–5114.

themselves can indeed be considered FA. In other words, their charged (ionizable amine groups) and nonpolar domains (olefin backbone and alkyl chain pendant group) reside on opposite sides of the bicyclic frame (Figure 1).

Overall, we found that these experimental methods (dye-leakage, DLS, microscopy, and ITC) using synthetic biomimetic vesicles provided new information on how SMAMPs interact with phospholipid membranes, revealing behavior different from that found in previous HDP studies. It was observed that the membrane is severely compromised by polymer-induced aggregation rather than some type of pore-induced leakage as seen with some HDPs or complete vesicle disruption in the presence of simple surfactants. Also it was demonstrated that synthetic vesicles model bacterial cells fairly well when studying the interactions of membrane-disruptive antimicrobial polymers. These experiments represent an important step in elucidating the modes of action of these bioactive polymers. Gaining a clearer understanding of membrane interactions, equal to that found in the HDP literature,³ will lead to better designs of membrane-interacting polymers.

Experimental Section

Materials. For polymerizations, Grubbs' third generation catalyst²¹ [(H₂Imes)(3-Br-py)₂(Cl)₂Ru=CHPh] was used in dry CH₂Cl₂ (Acros, bottle sealed under nitrogen with molecular sieves). Chloroform solutions of phospholipids were obtained from Avanti Polar Lipids. Vesicles for dye-leakage, DLS, and ITC studies were constructed of POPE (1-palmitoyl-2-oleoyl-*sn*-glycero-3-phosphoethanolamine) and POPG lipids (1-palmitoyl-2-oleoyl-*sn*-glycero-3-[phospho-*rac*-(1-glycerol)] sodium salt). Calcein dye and Triton-X (polyoxyethylene isooctylphenyl ether) were obtained from Aldrich. Vesicles for the fluorescence microscopy studies were constructed of *E. coli* lipid extract, from Avanti Polar Lipids, with rhodamine labeled lipids (1,2-dipalmitoyl-*sn*-glycero-3-phosphoethanolamine-*N*-[lissamine rhodamine B sulfonyl] ammonium salt). SYTO9 dye for staining bacteria was obtained from Invitrogen. Tris-saline buffer (10 mM Tris, 150 mM NaCl, pH ~7) was used in all experiments.

Instrumentation. Gel permeation chromatography (GPC) was performed on the Boc-protected polymers with a Polymer Laboratories LC1120 pump equipped with a Waters differential refractometer detector. The mobile phase was THF with a flow rate of 1.0 mL/min. Separations were performed with 105, 104, and 103 Å Polymer Laboratory columns and molecular weights were calibrated versus narrow molecular weight polystyrene standards. For HPLC studies, a Waters 2695 Separation Module HPLC system was used and equipped with a Waters 2996 photodiode array and an Agilent Zorbax C8 column (150 mm length). For polymer-induced dye-leakage studies, fluorescence was recorded with a Perkin-Elmer LS50B luminescence spectrometer (Ex. = 490 nm and Em. monitored = 515 nm). For DLS experiments, a commercial laser light scattering spectrometer was used that contained an ALV 5000 correlator. ITC experiments were performed on a VP-ITC microcalorimeter from Microcal. Fluorescence microscopy images were taken on an Olympus BX51 Reflected Fluorescence Microscope (Optical Analysis Corp.) equipped with a 100 W Mercury Lamp (Chin Technical Corp.).

Preparation of Polymers. The synthesis and characterization of polymers 1–4 has been reported before.¹ Briefly, a typical

polymerization for 1–3 involved adding 5 mL of dry CH₂Cl₂ to a N₂ purged test tube containing Boc-protected monomer (1.5 mmol) plus Grubbs' third generation catalyst (0.05 mmol).²¹ The N₂ line was removed and the solution was stirred at 30 °C for 30 min after which 0.5 mL of ethyl vinyl ether was injected and the solution stirred for 15 min to terminate the polymer. This solution was added dropwise to 500 mL of stirring pentane to precipitate the polymer. The precipitate was then collected by a fine sinter funnel, redissolved, and precipitated again then dried under vacuum. Polymer 4 required modified reaction conditions of 60 min stirring in distilled THF at 60 °C to obtain 100% conversion.

The resulting Boc-protected polymers were soluble in THF, and GPC (calibrated to polystyrene) was used to approximate *M_n* of the Boc-protected polymers and polydispersity index (PDI). Previous studies indicated that GPC derived weights match closely the weights derived from NMR analysis of the deprotected (TFA-salt) forms of the polymers (TFA = Trifluoroacetic acid). All polymers afforded monomodal GPC traces with PDIs between 1.05 and 1.11. The *M_n* for each polymer was determined (1 = 9600 g/mol, 2 = 8900 g/mol, 3 = 12100 g/mol, 4 = 10,600 g/mol). These *M_n* values corresponded to polymers with an average degree of polymerization (DP) of 31, 26, 33, and 27 units for 1–4, respectively.

The Boc-protected polymers were deprotected by stirring 100 mg in 8 mL of 1:1 TFA/CH₂Cl₂ for 2 h. The solutions were dried to an oil using a rotary evaporator set at 40 °C and placed under vacuum for 2 h. Finally, the solids were fully dissolved in 4 mL MilliQ water and freeze-dried for 48 h to give eggshell colored soft solids. NMR spectra in DMSO-*d*₆ confirmed complete removal of the Boc protecting groups and matched literature spectra.¹ Polymers 1–3 gave clear solutions in Tris-saline buffer (10 mM Tris, 150 mM NaCl, pH ~7) at concentrations of 8 mg/mL and lower. Polymer 4 showed limited solubility in this buffer but was fully soluble in DMSO.

Reverse-Phase HPLC Analysis. The aqueous phase was 0.1 vol % TFA in water while the organic phase was 0.1 vol % TFA in CH₃CN. Both solvents were filtered then degassed by sonication for 30 min. Solutions of polymer (1 mg/mL in a 1:1 mixture of aqueous/organic solvent) were eluted off of the column using a mobile phase gradient that started at 99% aqueous held for 5 min then ramped down to 20% aqueous over 40 min. Flow rate was 1 mL/min and absorbance at 212 nm was monitored.

Preparation of Biomimetic Vesicles. The following is a general procedure to make dye-loaded large unilamellar vesicles (LUVs). Chloroform solutions of POPE (3.23 mg, 0.0045 mmol) and POPG (1.15 mg, 0.0015 mmol) were mixed in a 10 mL round-bottom flask and the chloroform was removed at room temperature by rotary evaporator to form a uniform film. The flask was placed under vacuum for an additional 6 h. The dried film was hydrated by vortex with 1 mL of a 40 mM aqueous calcein dye solution in Tris buffer, minus the NaCl, and adjusted to pH 7. The solution was subjected through five freeze/thaw cycles using liquid nitrogen and warm water. All 1 mL of solution was subjected to extrusion (a total of 15 passes) through two stacked 400 nm pore PC membranes (Avanti Polar Lipids) at room temperature. Finally, the solution was passed through a column packed with Sephadex-25 (Sigma-Aldrich) eluting with Tris-saline buffer to separate dye-loaded vesicles from nontrapped calcein dye. Fractions (~5 drops each) were collected. Vesicle solutions were stored in a vial at 4 °C and diluted as needed for up to 4 days.

LUVs for DLS and ITC studies were prepared as described above except the film was hydrated with 1 mL of Tris-saline buffer and not 1 mL of calcein solution. Additionally, after extrusion through a 400 nm pore membrane, a Sephadex column was not necessary since there was no nontrapped dye to remove. This 1 mL stock of vesicles had a lipid concentration of 6 mM (equal to 4.38 mg or 6 μmol).

Vesicles for the fluorescence microscopy studies were made from a lipid film of 5 mg of *E. coli* lipid extract and 0.005 mg of the Rhodamine labeled lipid. This film was subjected to the same hydration process as for the nondye-loaded LUVs. Extrusion through a membrane was not performed to keep the vesicles much larger

(15) Arnt, L.; Nüsslein, K.; Tew, G. N. *J. Polym. Sci., Part A: Polym. Chem.* **2004**, *42*, 3860–3864.

(16) Kuroda, K.; DeGrado, W. F. *J. Am. Chem. Soc.* **2005**, *127*, 4128–4129.

(17) Schmitt, M. A.; Weisblum, B.; Gellman, S. H. *J. Am. Chem. Soc.* **2004**, *126*, 6848–6849.

(18) Mowery, B. P.; Lee, S. E.; Kissounko, D. A.; Epand, R. F.; Epand, R. M.; Weisblum, B.; Stahl, S. S.; Gellman, S. H. *J. Am. Chem. Soc.* **2007**, *129*, 15474–15476.

(19) Sambhy, W.; Peterson, B. R.; Sen, A. *Angew. Chem., Int. Ed.* **2008**, *47*, 1250–1254.

(20) Arnt, L.; Tew, G. N. *Langmuir* **2003**, *19*, 2404–2408.

(21) Love, J. A.; Morgan, J. P.; Trnka, T. M.; Grubbs, R. H. *Angew. Chem., Int. Ed.* **2002**, *41*, 4035–4037.

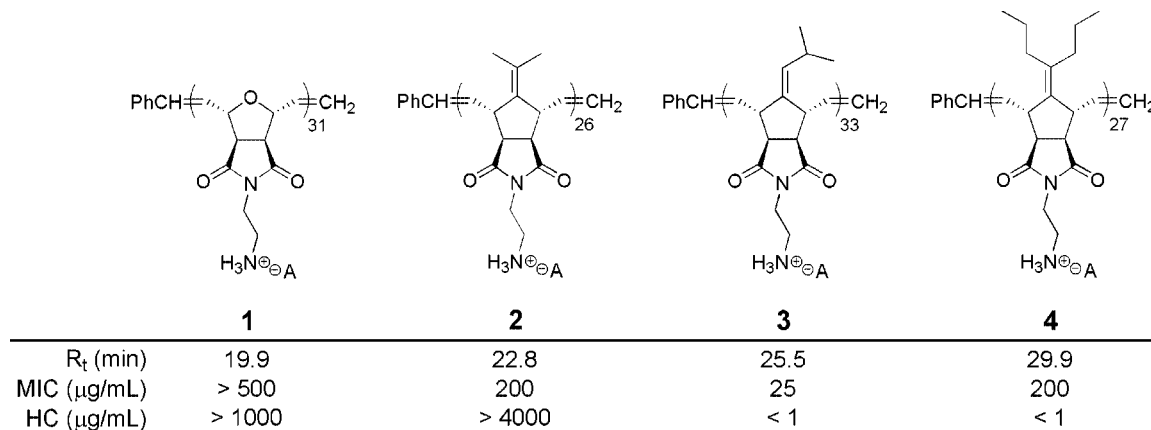


Figure 1. Polymers studied and their retention time (R_t) on a reverse-phase HPLC column. The counteranion was trifluoroacetate. MIC (against *E. coli*) and HC values were previously reported.¹

(and thus visible by microscopy) than vesicles passed through a 400 nm pore membrane.

Polymer-Induced Leakage of Vesicles. Vesicle fractions were diluted 6-fold and 25 μL of this stock solution was added to 2 mL of Tris-saline buffer. The diluted fractions that afforded a fluorescence intensity of <80 au before addition of polymer and a fluorescence intensity >800 au at 100% dye-leakage exhibited a useful intensity range and were used. Triton-X (20 $\mu\text{g/mL}$ final concentration) was used as the strong surfactant to induce complete vesicle disruption and was considered to release 100% of the dye for comparison to polymer-induced leakage.

In a typical experiment, 25 μL of the chosen diluted fraction was added to 2 mL of Tris-saline buffer and an intensity of <80 au was confirmed. A solution of polymer was added (2 $\mu\text{g/mL}$ final concentration) and the solution was agitated with the pipettor tip and placed in the spectrometer a couple of seconds after polymer addition. Emission at 515 nm was monitored and recorded with time. After 15 min Triton-X was added and the corresponding fluorescence was taken as 100% leakage.

Dynamic Light Scattering. DLS measurements were taken in 5° angular increments from 35° to 65° for 10 s at each angle for a total of 20 min. For a typical experiment, a 2 mL solution of LUVs (42 μM was the final lipid concentration, diluted from the extruded 1 mL stock) in Tris-saline buffer was monitored via DLS at 25 °C and allowed to equilibrate in a xylene bath for approximately two minutes. Polymer was then added (25 μL of a 0.45 mg/mL solution) to the vesicle solution and agitated briefly with the pipettor tip and measurements started.

The field correlation function was recorded at various angles. A CONTIN analysis was used to fit the field correlation function. Fitting the relaxation rate versus the scattering angle yielded the diffusion coefficient. Applying the Stokes–Einstein relationship, a hydrodynamic radius, R_h , was determined. For each polymer five trials were performed and averaged. Solutions of polymer alone or polymer/vesicle solutions with added Triton-X (2 $\mu\text{g/mL}$ final concentration) did not provide the signals characteristic of formation of aggregates that can be measured by DLS.

Fluorescence Microscopy of Vesicles and *E. coli*. Vesicles composed of *E. coli* extract lipids with a 1 wt % of Rhodamine labeled lipid were used for the fluorescence microscopy studies of polymer/vesicle binding. The extrusion step was skipped so that the vesicles remained much larger (and therefore within the resolution limit of microscopy) than the ones used for the vesicle dye-leakage, DLS, and ITC experiments.

In a typical experiment for the vesicle trials 40 μL from the 1 mL of vesicle stock solution was added to 2 mL of Tris-saline buffer. All four polymer stock solutions were made in DMSO at 2 mg/mL and 5 μL of this solution was added to the diluted vesicle solution. After sitting undisturbed for 30 min, 50 μL of the polymer/vesicle solution was deposited on a microscope slide and covered by a

coverslip. Vesicles were viewed under a red filter (Ex. = 480–550 nm, Em. = 590–800 nm).

For imaging *E. coli*, 500 μL of a solution of bacteria (diluted to 10^8 cells with Tris-saline buffer) was incubated at room temperature with SYTO9 dye for 15 min. Then 7.5 μL of a 5 mg/mL DMSO solution of polymer was added to 500 μL of this stained bacteria solution. After another 30 min of incubation, 50 μL of the polymer/bacteria solution was deposited on a microscope slide and covered by a coverslip. Images were taken of the bacteria, viewed under a green filter (Ex = 420–480 nm, Em = 520–800 nm).

Isothermal Titration Calorimetry. All solutions were made in Tris-saline buffer that had been previously degassed for 30 min by sonication. For a typical ITC run the instrument chamber contained a solution of vesicles (0.30 mM in lipids) while a 0.45 mg/mL solution of polymer (equivalent to ~0.047, 0.051, 0.037, 0.042 mM for 1–4, respectively) was taken up in the 250 μL injection syringe. The syringe was assembled into the chamber for equilibration while stirring at 260 rpm. The baseline heat signal (set at 10 $\mu\text{cal/sec}$) and chamber temperature (set at 27 °C) usually stabilized within 5–10 min before a first injection of 3 μL was performed. (This first data point was not included in the analysis as recommended by Microcal) The next 20–25 injections (enough to be reach saturation) were 9.3 μL each added over 18 s and spaced 5 min apart.

ITC runs of polymer added to buffer, and buffer added to vesicles were also performed and gave negligible heats. ORIGIN software was used to fit the results from which entropy, enthalpy, and binding stoichiometry could be obtained. Experiments were performed in duplicate on different days with freshly made polymer and vesicle solutions.

Results and Discussion

HPLC. To rank the relative hydrophobicity of the SMAMPs used in this study, reverse-phase high-performance liquid chromatography was performed.²² Analysis showed that as the size of the nonpolar pendant group became larger, the apparent hydrophobicity of the polymer increased (Figure 1) as evidenced by the longer retention times on a C8 reverse-phase column. Also, retention times were fairly insensitive to the size of the polymer. For instance, the retention time of 1 at 15.1 kDa was about 0.7 min longer than a shorter chain of 1 at 3.3 kDa. We therefore believe that the HPLC experimental parameters are near the critical condition.²³

In the field of SMAMPs, the beauty of exploiting polymer chemistry with a set of carefully chosen monomers is that a diverse series of compounds, at various molecular weights, can

(22) Schmitt, M. A.; Weisblum, B.; Gellman, S. H. *J. Am. Chem. Soc.* **2007**, *129*, 417–428.

(23) Pasch, H.; Trathnigg, B. In *HPLC of Polymers*; Springer-Verlag: Berlin, 1999.

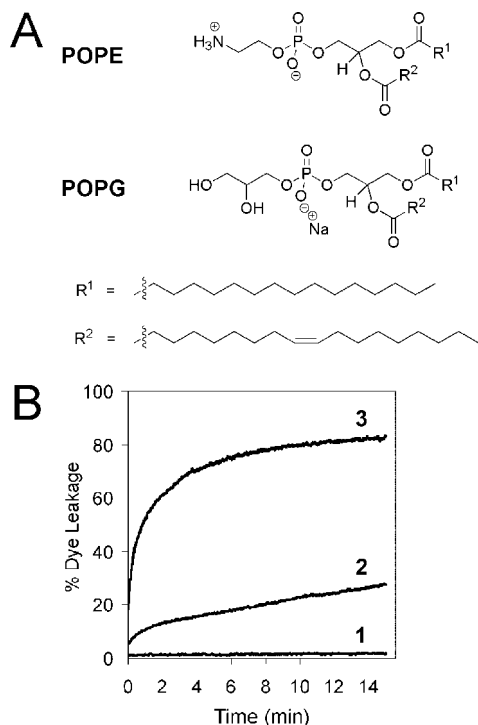


Figure 2. (A) Structures of POPE and POPG phospholipids used to form large unilamellar vesicles (LUVs) for vesicle leakage, DLS and ITC studies. (B) Induced leakage profiles of dye-loaded vesicles ($\sim 12 \mu\text{M}$ in lipids) upon addition of polymer ($2 \mu\text{g/mL}$).

be conveniently accessed.^{1,16} Previously, **1–4** were shown to possess a remarkable range of antimicrobial and hemolytic activities (Figure 1). Additionally, these activities were independent of molecular weight,¹ which was in contrast to other antimicrobial polymer systems reported.^{16,24} Antimicrobial activity using a minimum inhibitory concentration (MIC) assay against *E. coli* and toxicity using a hemolytic concentration (HC) assay against human red blood cells were assessed in a previous report.¹ It was shown that the most hydrophilic polymer, **1**, was the least potent against bacteria (MIC was highest among the four) and it did not lyse human red blood cells (HC also was highest among the four). In contrast, the most hydrophobic polymer, **4**, showed some antimicrobial activity but was extremely hemolytic indicating a high level of toxicity for humans. Low hemolytic activities will be essential for polymers that will be used to make indwelling devices such as cardiovascular and orthopedic implants permanently sterile.^{12,13} It was interesting that the more potentially useful polymers were in the middle of the hydrophobicity scale. Polymer **3** was the most potent with an MIC of $25 \mu\text{g/mL}$ but was also toxic, while **2** showed some antimicrobial activity with very favorable HC values.

Disruption of Phospholipid Vesicles. Large unilamellar vesicles (LUVs) were used to determine if these polymers were able to disrupt membranes. These LUVs were filled with a self-quenching dye, calcein, and polymer-induced dye-leakage was monitored. The LUVs were composed of a 3 to 1 ratio of zwitterionic POPE lipids and anionic POPG lipids (Figure 2A) in order to closely mimic the phospholipid composition of *E. coli* membranes.^{10,25}

While the membrane-disruption activities of **1–3** were monitored, **4**, was only partially soluble in Tris-saline buffer at

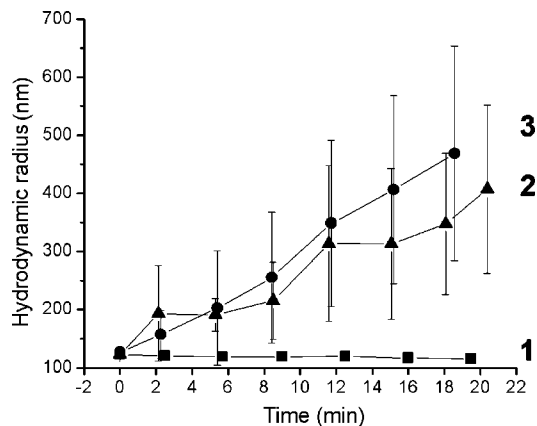


Figure 3. Graph of the change in hydrodynamic radius of aggregates, via DLS, upon addition of polymer ($5.6 \mu\text{g/mL}$) to a solution of vesicles ($42 \mu\text{M}$ in lipids).

pH 7 and was therefore not investigated by vesicle dye-leakage studies. Polymer **3** caused significantly more leakage than **2**, while **1** caused no observed dye-leakage (Figure 2B). These results followed the general trend of **3** being the most active against bacteria and were consistent with **3** having a mode of action related to membrane disruption. Also the antimicrobial inactivity of **1** was mirrored by the dye-leakage studies showing no apparent membrane-disruption. Thus HPLC, the biological assays (MIC and HC), and the LUV studies were fully self-consistent.

It was noticed, in concentration variable studies, that 100% dye leakage could not be reached even by doubling the amount of **3** added or with longer times. Similar results, in which leakage does not go to completion, have been observed for the HDP Magainin,²⁵ antimicrobial proteomimetics,²⁶ and short antimicrobial oligomers.²⁵ This result suggested that some dye was permanently trapped and complete vesicle lysis did not occur. Although these polymers were shown to be membrane-disrupting agents, a deeper understanding of the fundamental mechanisms by which they interact with phospholipid membranes was desired.

Interactions Observed by Dynamic Light Scattering. While induced leakage of dye-loaded vesicles is a standard method to show membrane-disruption activity, DLS, to our knowledge, had never been employed to probe the nature of the interactions between vesicles and SMAMPs. The HDP literature contains a useful DLS study on gramicidin S.⁵ It was shown that this HDP caused little change in the biomimetic vesicle diameter and the authors concluded that this was consistent with insertion of the peptide into the membrane.

For our study, the hydrodynamic radius (R_h) of the vesicles was monitored in the presence of polymer in a high salt (150 mM) environment. The R_h was determined at different time points and plotted (Figure 3). Each trial started with confirmation that the vesicles alone gave a consistent R_h value, in this case 125 nm. Although a 400 nm diameter pore membrane was used to prepare these vesicles, it was reasonable that extrusion would produce vesicles somewhat smaller than the pore. Also confirmed was that polymer alone, at the experimental conditions, did not form large polymer aggregates to any significant extent.

Upon addition of SMAMP **2** or **3** to a vesicle solution, it was observed that the vesicles clearly aggregated, reaching the upper measuring range limit of the instrument ($R_h = 500 \text{ nm}$) (Figure 3). This dramatic growth occurred within 20 min. Addition of the surfactant, Triton-X, caused complete vesicle disruption

(24) Tew, G. N.; Clements, D.; Tang, H.; Arnt, L.; Scott, R. W. *Biochim. Biophys. Acta, Biomembr.* **2006**, *1758*, 1387–1392.

(25) Som, A.; Tew, G. N. *J. Phys. Chem. B* **2008**, *112*, 3495–3502.

(26) Liu, D.; DeGrado, W. F. *J. Am. Chem. Soc.* **2001**, *123*, 7553–7559.

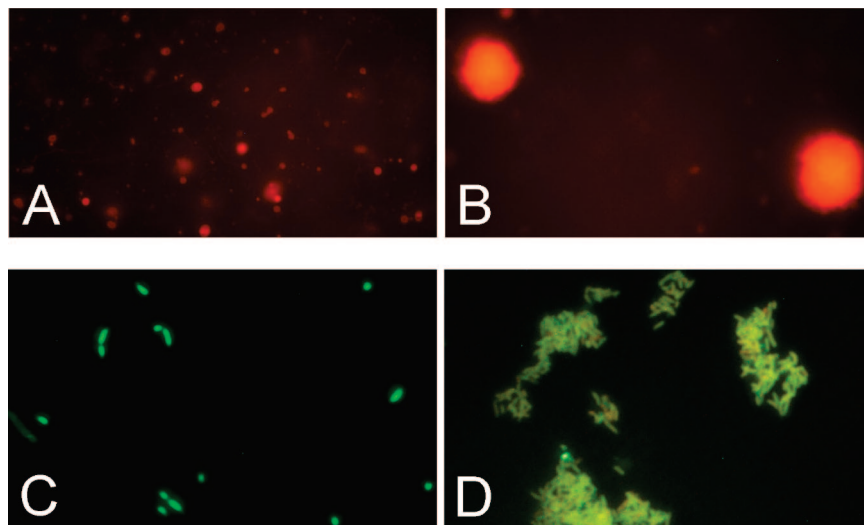


Figure 4. Fluorescence microscopy. (A) Rhodamine labeled vesicles formed from *E. coli* lipid extracts before addition of polymer and (B) after 30 min in the presence of polymer **3**. Vesicles had an approximate diameter of 2–3 μm . (C) Stained bacteria (*E. coli*) before addition of polymer and (D) after 30 min in the presence of polymer **3**. Bacteria were \sim 1–2 μm in length.

showing that this detergent can effectively break-up vesicle aggregates as well as individual vesicles. Interestingly, the polymer with the lowest antimicrobial activity, **1**, did not aggregate the vesicles. This finding suggests the importance of the alkyl side group of **2** and **3** to effect any stable interaction with the vesicle membrane. The amount of ionizable amine groups for each polymer was approximately the same and thus it appeared that electrostatic attraction, alone, between the cationic polymer and anionic vesicles was not sufficient to display any observable interaction.^{25,27}

While it appeared that the vesicle aggregation ability shown by DLS did not differentiate **2** from **3** to the same extent that the biological and dye-leakage studies did, DLS provided a clearer picture of polymer/vesicle interactions for these SMAMPs than was known prior to this study. The active polynorbornenes **2** and **3** lead to aggregated vesicles, rather than solely form pores as supposed with gramicidin S.⁵ Thus, these polymers, although cationic and amphiphilic, did not display detergent-like action, where they would lyse the membrane and completely solubilize it so that no aggregates would exist. Instead they acted as a glue where the polymer was able to capture many vesicles, which attracted other polymer chains, eventually leading to a tangled aggregate (see below).²⁸

Visualization of Fluorescent Vesicles and Bacterial Cells.

Fluorescence microscopy was used to visualize vesicles and stained bacteria after incubation with polymer solutions (Figure 4). Vesicles composed of *E. coli* extract lipids were labeled with 1 wt % Rhodamine tagged lipids. These vesicles were not extruded through a membrane and therefore these giant multilamellar vesicles were large enough to be seen under the microscope. It was observed that before addition of polymer, the vesicles appeared fairly spherical and had an average diameter of about 2–3 μm (Figure 4A). After adding a solution of **3** and letting the mixture sit for 30 min, the vesicles appeared to have grown to greater than 10 μm in diameter (Figure 4B).

Fluorescence microscopy was also performed with stained bacterial cells. *E. coli* was stained with a green-emitting, fluorescent SYTO9 dye (Invitrogen) that can penetrate and stain the DNA of live cells. In the absence of polymer, cells appeared

as bright ovals about 1–2 μm in length (Figure 4C). However after a 30 min incubation period with **3** at a 75 $\mu\text{g/mL}$ concentration, the morphology visually changed (Figure 4D). There were only a few bright cells visible and they seemed to be embedded in a cluster of supposed cellular material where the outlines of intact cells did not exist. Additionally, the intensity of the fluorescence was dimmed in these areas of bunched cellular material probably due to the dispersion of dye. Thus, these results supported that **3** interacts with, and compromises, the cellular membrane of bacteria, which corroborates the antimicrobial studies. Further, they supported the conclusion from DLS that the polymers induce aggregation of membranes.

Interactions Observed by Isothermal Titration Calorimetry.

To obtain information about the energetics of polymer/vesicle binding, ITC isotherms were collected at 300 K. Polymer solution was added, using timed multiple injections, to a reservoir of vesicles (Figure 5). Similarly to DLS, ITC studies have also been informative in the field of HDPs^{6,8} but we are unaware of ITC investigations of binding between vesicles and SMAMPs.

As might be expected, **1** did not exhibit any appreciable heats evolved or absorbed during the titration, indicating that no apparent net binding to vesicles occurred. Therefore, just like in the DLS studies, it appeared that when mixed the energetics of the system dictated that polymer **1** and vesicles remain isolated from each other. Polymer **4** gave a slightly turbid solution in buffer but was nonetheless also studied by ITC.²⁹ In the titration with **4**, there appeared to be some molecular process, possibly polymer deaggregation, taking place. Still, the amount of heat associated with this process was minimal as evidenced by the integrated area of each heat signal. The process may also be a combination of polymer deaggregation along with lipid binding such that when these heats were summed, it resulted in near zero heats.

On the other hand, injecting a solution of **2** or **3** into a solution of vesicles resulted in a clearly sigmoidal binding curve in which the process was overall endothermic. Line-fitting to a “one site” model, provided by the Microcal software, that adjusts free energy (ΔG), enthalpy (ΔH), entropy (ΔS), and most importantly binding stoichiometry, indicated that the binding of polymer **2** or **3** to

(27) Yang, L.; Gordon, V. D.; Mishra, A.; Som, A.; Purdy, K. R.; Davis, M. A.; Tew, G. N.; Wong, G. C. L. *J. Am. Chem. Soc.* **2007**, *129*, 12141–12147.

(28) Menger, F. M.; Seredyuk, V. A.; Yaroslavov, A. A. *Angew. Chem., Int. Ed.* **2002**, *41*, 1350–1352.

(29) Turbidity caused by **4** would have scattered too much light in the DLS studies relative to the vesicles. Plus, the ITC instrument allows continuous stirring, unlike the DLS setup, thus possibly promoting dissolution of **4** especially in the presence of lipid binding partners to break up polymer aggregates.

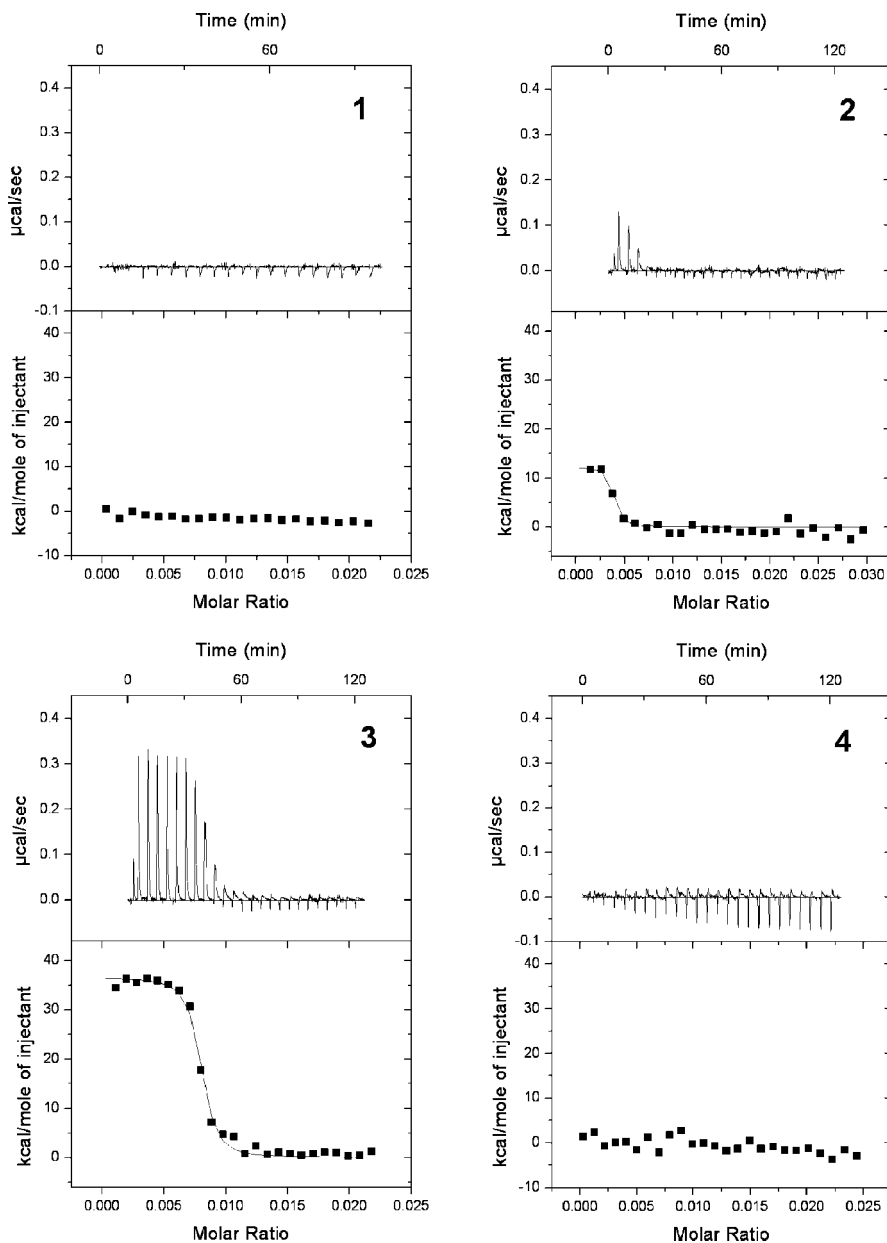


Figure 5. Representative binding isotherms obtained by the titration of a vesicle solution (300 μM in lipids pretitration) with a polymer solution (9.3 μL per injection of a 450 $\mu\text{g}/\text{mL}$ solution). Temp = 300 K. Top panels show heat pulses (endothermic) per injection of polymer. Bottom panels are the corresponding integrated areas (squares) and the line-fitted isotherm curve (in titrations using **2** or **3**). Y-axes for each isotherm are on identical scales and molar ratios on the X-axes are concentration ratios, [polymer]/[lipids].

vesicles is entropically favorable. At the same time, ΔH was found to be positive, thus unfavorable for both polymers (36 and 12 kcal/mol for **3** and **2**, respectively), while ΔS was extremely favorable and dominant in the binding process (156 and 76 cal/mol·K for **3** and **2**, respectively). An entropically favorable process can be attributed to the entropy gain of released counterions and/or liberated solvent molecules when two hydrophobic regions come in close contact, thus releasing solvents and small ions. This collapse of sufficiently hydrophobic domains to exclude water may explain why cationic **1** showed no net binding to anionic vesicles. Though electrostatic attraction between a positively charged polymer and anionic vesicle would be expected, **1** does not have the necessary hydrophobic regions to bury within the nonpolar interior of the lipid bilayer thus stabilizing polymer/vesicle interactions. Similarly, polymer **4**, which is the most hydrophobic aggregates strongly with itself instead of inserting into the vesicle bilayer.

The calculated free energy of binding was favorable, and unexpectedly, nearly identical for vesicle binding by **2** and **3** ($\Delta G = -10.8$ and -10.6 kcal/mol, respectively). In contrast, their binding stoichiometries, or the molar ratios at the inflection point, (Figure 5) was significantly different between the two polymers. One would expect that the binding area (essentially the vesicle surface area) is identical whether **2** or **3** is added, which would therefore lead to the prediction that any dissimilarities in binding would be a result of different binding strengths (ΔG) rather than binding stoichiometry (molar ratio). However, this was not the case. From the line-fits, the binding stoichiometry (molar ratio = [polymer]/[lipid]) was about 0.0038 for **2** and 0.0080 for **3** (Figure 5). According to literature, a 250 nm diameter phospholipid vesicle (approximately the size of the vesicles used here based on DLS) contains about 550 000 lipid molecules.³⁰ Converting the above molar ratio to the number of polymer chains per vesicle calculated ~ 2090 molecules of **2** bound to every

vesicle whereas every vesicle was calculated to be bound by an average of 4400 molecules of **3**.

Of course, 4400 chains of **3** draped around an intact vesicle is an overly simplified picture, if not an inaccurate one. This depiction does not take into account vesicle disruption where it is assumed that all the lipids, even lipids in the inner leaflet of the bilayer would eventually be exposed and available for binding by polymer. This scenario appeared to be even more likely when the binding ratio above (based on the number of polymers per vesicle) was converted to the number of polymer cationic charges per anionic lipid. Recalling that a 3:1 zwitterionic to anionic lipid composition was used for the vesicles, this would mean that 137 500 lipids would be anionic per vesicle while polymer **3** has an average of 33 ionizable amine groups and **2** has 26 (Figure 1). Therefore, the cationic amine-to-anionic lipid ratio for **2** would be 0.40 but for **3** it would be 1.06, a near 1:1 correlation. DeGrado and co-workers have taken a similar approach of considering the total number of lipids bound per cationic peptide in their analysis of vesicle binding and found a ratio near unity as well (1.15–1.19).²⁶

Therefore, for this particular system, it is noteworthy that binding stoichiometry, and not binding strength, was a qualitative predictor of antimicrobial activity, where the most bioactive polymer, **3**, was also the one that vesicles attract the most. When thinking generally about the events during an MIC assay, we speculate that a threshold amount of polymer is required to bind to the membrane to trigger any antibacterial activity. For **3** this bound polymer threshold is surpassed at low concentrations thus leading to a lower MIC value. Due to the “nature” (chemical structure, amphiphilicity, solution dynamics, etc.) of **2**, this threshold is presumably not reached in the biological assays until concentrations much higher as compared to assays using **3**.

Conclusions

In combination, dye-leakage studies, DLS, ITC, and fluorescence microscopy on vesicles and bacterial cells support that the antimicrobial polynorbornenes studied here interact with phospholipid membrane surfaces. This interaction led to extensive aggregation but it appeared that complete membrane disruption did not take place as it would happen with other surfactants. Nor did this membrane interaction appear to form pores as has been observed with some membrane-interacting HDPs.

(30) Menon, A. K. In *Methods in Molecular Biology*, vol. 228, 271–278. Gummadi, S. N.; Hrafnisdottir, S.; Walent, J.; Watkins, W. E.; Menon, A. K. In *Membrane Protein Protocols: Expression, Purification, and Crystallization*, Selinsky, B. S. (Ed.), Humana Press series ‘Methods in Molecular Biology’, 2002, 228: 271–279.

DLS and ITC have been used effectively before to elucidate the mechanism of antimicrobial peptides but have not been adopted by the relatively young but quickly expanding field of SMAMPs. Here, we have shown the utility of DLS and ITC to reveal greater information into the membrane activities of antimicrobial polymers. In particular, DLS indicated aggregation events that did not lead to detergent-like dissolution of the lipid bilayer. While ITC revealed that even though binding strengths (ΔG) of the active, but biologically distinct, **2** and **3** were near identical, the binding stoichiometries were quite different. Additional studies on membranes analogous to those used here are currently being explored.^{9,31} Last, fluorescence microscopy demonstrated the similarities between using model vesicles and live bacterial cells.

In terms of future molecular design, it was clearly shown that cationic polymers do not substantially interact with anionic vesicles unless there is a significant hydrophobic component to stabilize this interaction. Recently, we reported the use of facially amphiphilic monomers as an extremely effective way to afford highly potent antimicrobial polymers that are entirely benign to mammalian red blood cells.³² Additionally, we have modified the design of polymer **1** to create guanidinium analogues that remain potentially antimicrobial but are not strongly membrane disruptive.³³ These new guanidinium analogs were also shown to efficiently transport a range of biological analytes through lipid bilayers.³⁴ It is envisioned that these types of SMAMPs will be useful for the production of permanently sterile materials especially those with intimate tissue contact such as biomedical implants.^{10,12,13}

Acknowledgment. We acknowledge the National Institutes of Health (RO1-GM-65803) and the Office of Naval Research (N00014-07-1-0520) for their generous support. Analytical facilities utilized in these studies were supported by the NSF-sponsored Materials and Research Science and Engineering Center on Polymers at UMass Amherst (DMR-0213695). We also thank Dr. Karen Lienkamp and Ms. Semra Colak for their DLS expertise in addition to invaluable comments on early drafts.

LA802232P

(31) Chen, X.; Tang, H.; Even, M. A.; Wang, J.; Tew, G. N.; Chen, Z. *J. Am. Chem. Soc.* **2006**, *128*, 2711–2714.

(32) Lienkamp, K.; Madkour, A. E.; Musante, A.; Nelson, C. F.; Nüsslein, K.; Tew, G. N. *J. Am. Chem. Soc.* **2008**, *130*, 9836–9843.

(33) Gabriel, G. J.; Madkour, A. E.; Dabkowski, J. M.; Nelson, C. F.; Nüsslein, K.; Tew, G. N. *Biomacromolecules*, **2008**, (DOI: 10.1021/bm800855t).

(34) Hennig, A.; Gabriel, G. J.; Tew, G. N.; Matile, S. *J. Am. Chem. Soc.* **2008**, *130*, 10338–10344.